CLEAR Anatomy and Physiology of the Anterior Eye Supplementary Appendix

2.3. Clinical assessment of corneal structure and function

A range of clinical instruments are available to assess corneal structure and function; herein, an overview of these techniques is provided.

2.3.1. Structure

2.3.1.1. Slit lamp biomicroscopy

Slit lamp biomicroscopy is the most common method used to assess the health of the anterior eye, including the cornea and limbus (see CLEAR Evidence-based Practice Report [1]), both direct and indirect illumination techniques are commonly used [2].

Sodium fluorescein and lissamine green are two vital dyes used commonly for ocular surface evaluation [3,4]. Each is typically instilled into the eye using a dye-impregnated paper strip [4–7] or in liquid form [5,6,8]. In healthy eyes, uptake of these dyes is limited by the epithelial glycocalyx [9]. Areas of ocular surface compromise tend to promote dye uptake, known as 'staining'. Several grading scales exist to support standardised assessments of staining severity including the van Bijsterveld [10], Cornea and Contact Lens Research Unit (CCLRU) [11], National Eye Institute (NEI) [5], Efron [12] and Oxford [6] scales. Sodium fluorescein, a water soluble dye that fluoresces yellow-green when excited by blue light (the optimal having a wavelength of 495nm [13]), is commonly applied to allow for the assessment of corneal staining and to evaluate rigid contact lens fittings. Sparse, punctate corneal fluorescein staining is likely physiological, occurring as a consequence of normal epithelial shedding; pathological corneal staining typically results in more extensive cellular damage and is associated with enhanced staining [9]. Ocular surface staining assessment is a key element of contact lens practice [14], and should be performed routinely to consider tissue changes related to factors such as hypoxia, trauma, inflammation, infection, toxicity and/or exposure.

The limbus should also be carefully evaluated, including a circumferential evaluation of the limbal vessels to consider any hyperaemia or corneal vascular encroachment. As the limbus houses the stem cell precursors of the corneal epithelium, it is important to note any impacts of contact lens wear. Limbal stem cell deficiency may occur as a consequence of contact lens wear, particularly with prolonged use [15–17] (see CLEAR Complications Report [18]).

Whilst a mainstay of anterior eye evaluation, slit lamp evaluation has some limitations, primarily related to resolution and the subjective nature of the assessment [19]. For these reasons, a range of additional technologies have emerged, as considered below.

2.3.1.2. Topography and tomography

The evaluation of corneal shape is another key component of contact lens practice. As reviewed by Fan et al. corneal topography and tomography are non-invasive clinical techniques for rapid derivation of corneal quantitative parameters [20].

Corneal topography is used to evaluate the shape and physical parameters of the anterior corneal surface. A common technique, which is dependent on tear film quality, involves projection of a Placido disc (set of illuminated concentric rings) onto the cornea, which is reflected and analysed to derive quantitative measures of anterior curvature [21]. Alternatively, Fourier transform profilometry is suggested for measuring corneal and scleral topography [22].

Compared with keratometry, which measures the curvature of the principal corneal meridia at only four locations, positioned 3 mm from the corneal apex (to derive measurements colloquially known as 'K-readings'), corneal topography allows for derivation of substantial additional information including: the limbal to limbal diameter, corneal eccentricity, peripheral corneal curvature, and quantitative shape indices (to identify conditions such as keratoconus). Corneal topography maps can be displayed in several formats. Axial (sagittal) maps are derived based upon the assumption that the centre of the radius of curvature coincides with the optical axis. Tangential (instantaneous) maps show the local radius of curvature, independent of the central axis and are useful for identifying localised changes in corneal curvature, including in keratoconus and for orthokeratology lens fitting. Corneal tomography involves a three-dimensional reconstruction of the cornea, from which anterior and posterior curvature, elevation and pachymetry data can be derived. Corneal tomography can be performed using optical coherence tomography (OCT), slit-scanning techniques or Scheimpflug imaging [20]. Typical values for corneal shape parameters are provided in Table 3 of the main paper.

2.3.1.3. Optical coherence tomography (OCT)

OCT is based on the principle of low-coherence interferometry [23]. Previous comprehensive reviews have considered OCT to evaluate anterior eye features [19] and for scleral lens fitting [24]; these topics are briefly considered here.

With capacity to provide high-resolution, cross-sectional corneal images, anterior segment OCT has been applied in the clinical evaluation and/or monitoring of a spectrum of conditions, including keratoconus [25], corneal dystrophies and degenerations [26], corneal grafts [27], ocular surface neoplasia [28] and dry eye disease [29]. In scleral lens fitting, OCT can inform initial trial lens selection, be used to assess the characteristics of the lens-eye interaction and be helpful to evaluate the ocular response to lens wear. OCT has further enabled enhanced understanding of anterior segment anatomy, including characteristics such as scleral thickness, curvature, toricity, and the anatomy of the corneoscleral junction [24].

2.3.1.4. *In vivo* confocal microscopy

IVCM, first described in 1988 [30], is a non-invasive imaging device that enables visualisation of the cellular components of the anterior ocular structures, in particular the cornea and limbus. IVCM has been applied to quantify a spectrum of corneal structural elements, including epithelial [31] and endothelial cell densities [32], sensory nerve parameters [33], keratocytes [34] and immune cells [35]. It is also valuable for identifying causative pathogens in infective keratitis, particularly fungal filaments and *Acanthamoeba* cysts [36,37], to guide therapeutic management.

Laser-scanning IVCM (Heidelberg Engineering Retinal Tomograph with the Rostock Cornea Module) is the most common clinical device [38,39]. The instrument has a maximum scan depth of 1500 µm, and a standard image size of 400 x 400 µm. Accurate quantification of corneal nerve parameters is dependent on multiple factors, including the IVCM device used, quality of image acquisition, image selection and sampling, and measurement method [40]. In view of these factors, normative quantitative criteria for corneal nerve parameters are not clearly established.

2.3.1.5. Specular microscopy

Specular microscopy is an established technique for evaluating the corneal endothelium. The specular microscope projects light onto the cornea and then captures the reflected image from the optical interface between the corneal endothelium and aqueous humour. The technique can also be used to identify changes in endothelial cell density (see Section 2.1.2.5 of the main report), and variability in endothelial cell shape. Polymegathism, involving a variation in cell size, represents a permanent change and has been suggested to indicate compromised endothelial cell function due to chronic hypoxia [41] (see CLEAR Complications Report [18] and CLEAR Scleral Lens Report [42]).

3.1.3. Clinical assessment of the conjunctiva

3.1.3.1. Slit lamp biomicroscopy

Similar to the cornea (see Section 2.3.1.1 of the main report), the conjunctiva is routinely examined using slit lamp biomicroscopy. Pictorial grading scales, such as the Efron scale [43,44], or photographic-scales, such as the CCLRU scale [11,45,46], can be used clinically to grade the conjunctival appearance in terms of hyperaemia and/or irregularity (e.g., formation of papillae). Automated measures of conjunctival hyperaemia are also available (e.g., JENVIS scale in the Oculus Keratograph 5M, OCULUS Optikgeräte GmbH [47]). A comprehensive examination is important for identifying abnormalities that may have implications for contact lens wear (see CLEAR Evidence-based Practice Report [1]). Although a complete discussion of such conditions is beyond the scope of this report, types of conjunctival pathology relevant to contact lens wear include degenerative (e.g., pterygium, pingueculum) and inflammatory conditions (e.g., conjunctivitis).

Another relevant conjunctival feature is lid-parallel conjunctival folds (LIPCOF), small folds in the infero-temporal and infero-nasal quadrants of the bulbar conjunctiva, parallel to the lower eyelid [48] (see CLEAR Complications Report [18]). It has been hypothesised that LIPCOF are formed due to increased shear forces between the bulbar and palpebral conjunctiva during blinking [49]. LIPCOF can be classified using a fold-height-based grading scale [48] or by counting the number of folds [50,51]. An increased number of LIPCOF has been associated with dry eye symptoms [4,48,52–55]. For LIPCOF sum (nasal + temporal LIPCOF) a cut-off value of ≥ 2 has been suggested to discriminate between normal and symptomatic dry eye patients [52]. LIPCOF can also interfere with tear flow and influence tear meniscus parameters [56,57].

3.1.3.2 Vital dyes and grading scales

While fluorescein is optimal for identifying corneal staining, lissamine green is more suited for conjunctival staining [58] (see CLEAR Evidence-based practice Report [1]). Lissamine green, which has similar surface staining properties to Rose bengal but with greater tolerability [59], highlights dead or degenerate conjunctival cells and cells unprotected by mucin or glycocalyx [60]; the dye penetrates cell membranes and stains cell nuclei [9]. A combination of fluorescein and lissamine green usefully provides simultaneous information on corneal, conjunctival and eyelid margin staining [58,61].

For lissamine green assessment, conjunctival evaluation should occur within one to four minutes of dye instillation, typically at 1% concentration using a volume of at least 25 µl [9]; dye fading can occur after this time period [9,60,62]. Lissamine green staining is observable as a green-blue punctate pattern on the conjunctival surface, with a diffuse white light. Visualisation of the staining pattern can be enhanced using a red barrier filter (Hoya 25A or Kodak Wratten Filter 92), which results in a black appearance to the staining pattern [6,60].

Several grading methods exist for quantifying conjunctival surface abnormalities; commonly used scales are the Oxford [6] and NEI [63], although none are considered a gold standard [3]. The Oxford scale [6] uses a logarithmic unit increase in the number of stained dots between grades (ranging from 0 to 5 in severity). The NEI scale [5], originally developed to quantify fluorescein staining, scores five zones of the cornea and six zones of the conjunctiva, from 0 to 3. As such, this scale sub-divides the nasal and temporal conjunctiva into superior paralimbal, inferior paralimbal and peripheral areas to enable the anatomical location of the staining to be recorded. Staining in either eye comprising more than nine conjunctival spots (lissamine green) or more than five corneal spots (fluorescein) is indicative of a positive result and a sign of tear homeostatic imbalance [4,64].

4.3. Clinical assessment of the eyelid and eyelashes

4.3.1. Structure

4.3.1.1. Slit lamp biomicroscopy

Examination of the eyelid structures, including the margins, meibomian glands, eyelashes, lid wiper region, and palpebral conjunctiva, is typically conducted using a slit lamp biomicroscope in clinical settings (see CLEAR Evidence-based Practice Report [1]). General observation and assessment of the eyelids and eyelashes is undertaken using low to medium magnification, and medium to high diffuse illumination. Detailed assessments are performed using higher magnification and illumination [2].

4.3.1.1.1. Eyelid appearance

The eyelids and their margins are one of the first structures to be examined in an anterior-to-posterior examination approach. Physical changes in eyelid appearance may include hyperaemia, telangiectasia (capillary dilation), hyperkeratinisation (often associated with ageing), rounding of the margin (associated with oedema and thickening), concretions (deposits of degenerated epithelial products) [65], and irregularity and notching (associated with the absorption of tissues near the meibomian gland orifices, and often an indicator of

chronic eyelid margin disease) [66–69]. A comprehensive summary of grading scales that can be used to classify these eyelid features is provided elsewhere [69].

4.3.1.1.2. Eyelashes

The eyelashes prevent the entry of debris into the eye and divert airflow away from the ocular surface [70]. Eyelash anomalies that can be detected during a thorough slit lamp examination include: (i) trichiasis: an abnormal misdirection of the eyelashes, such that they turn inward and may come into contact with the conjunctiva or cornea [71]; (ii) poliosis: a loss of eyelash pigmentation, such that they appear grey or white [71]; and (iii) madarosis: loss of eyelashes that may be associated with several ocular conditions [72] or obsessive-compulsive [73] disorders. Loss of eyelashes can also occur as a result of alopecia areata [74] and secondary to chemotherapy [75].

The eyelashes may show an accumulation of debris or crusting that could be due to Staphylococcal blepharitis (brittle scales/flakes) [76], seborrheic blepharitis (greasy scales/flakes) [77], *Demodex* blepharitis (cylindrical cuffs at base of lashes) [78,79] or pediculosis (louse, crabs, translucent oval nits) [80]. A comprehensive summary of eyelash diseases is provided elsewhere [71].

4.3.1.1.3. Palpebral conjunctiva

The palpebral conjunctiva can be clinically inspected after everting the superior and inferior eyelids. Roughness may be appreciated by observing the specular light reflection from the surface of the palpebral conjunctiva using white light illumination [81], or by instilling fluorescein and observing the features under blue illumination and a yellow barrier filter [82,83]. The clinical severity of the papillary response may be evaluated using a number of grading methods [12], however the Efron and CCLRU scales are reportedly the most commonly used [84].

4.3.1.1.4. Eyelid margin and lid wiper

Clinical assessment of the eyelid margin and lid wiper are described below.

4.3.1.1.4.1. Lid wiper epitheliopathy

Frictional interaction between the lid wiper and anterior surface of the eye (or contact lens) is thought to give rise to a condition known as lid wiper epitheliopathy (LWE) [85] (see CLEAR Material Impact Report [86]). To visualise LWE, vital dyes are instilled into the eye, typically twice over a three to five minute period, and the eyelid is everted (with care to avoid contact with the eyelid margin during eversion) and the extent of staining is evaluated and graded. As previously summarised, a variety of staining protocols have been described [87], including a combination of fluorescein and rose bengal [85,88], fluorescein and lissamine green [89],

fluorescein only [90] and lissamine green only [91]. An optimal protocol for LWE identification has recently been described, involving instillation of two drops of lissamine green (one minute apart), and observed one to five minutes later; or two drops of fluorescein (one minute apart), and observed three to five minutes later [92]; further details are provided in the CLEAR Evidence-based Practice Report [1]).

Several grading methods exist to evaluate the staining. It is typically recommended that both the extent (length in mm) and width (percentage of lid wiper region) of staining be evaluated along both the superior and inferior eyelids [88]. LWE is indicated by staining that is 2 mm or more in length, and/or involves at least 25% of the sagittal width (excluding the line of Marx) of the lid wiper [4]. With respect to contact lens wear, there remains some debate about the clinical significance of LWE. Some studies have associated LWE with ocular symptoms in contact lens wearers and non-contact lens wearers [91,93], whereas others have failed to observe a similar relationship [94,95].

4.3.1.1.4.2. Position of the mucocutaneous junction [Marx's line]

The mucocutaneous junction can be readily visualised along the inferior eyelid margin by instilling lissamine green [96–99], fluorescein [96,100], or rose bengal [96]. A change in the regularity of the line and a gradual anterior shift has been described in older individuals [101], meibomian gland dysfunction (MGD) [96], and blepharitis [101]. A grading scale can be used to evaluate the anterior shift of the mucocutaneous junction relative to the meibomian gland orifices [96].

4.3.1.2. Tarsal glands [meibomian glands]

Assessment of meibomian gland structure and function is an essential component of an eyelid examination [69,102], and is summarised below.

4.3.1.2.1. Assessment of the gland orifices

Examination of the meibomian gland orifices has a primary focus on the identification of MGD. In MGD, a range of morphological changes to the orifices occur [66,69]. Changes to gland orifices that may be observed [66,69], include: (i) altered numbers: duplicated or reduced; (ii) capping: a dome of oil solidified over the orifice; (iii) pouting: orifices slightly elevated above the eyelid margin, such that they are no longer flush with the margin due to obstruction and extrusion of plugs, consisting of lipids and keratinised cell debris; (iv) retroplacement: orifices dragged posteriorly due to cicatricial changes in the marginal mucosa, which may also expose the ducts; and (v) obliteration: orifices narrowed completely and expression of meibum is no longer visible; this may be accompanied by scarring, opaque orifices, loss of orifice definition and/or vascular invasion [66,69].

4.3.1.2.2. Meiboscopy and meibography

Meiboscopy and meibography (Figure 14 of the main CLEAR Anatomy Report) refer to *in vivo* visualisation and imaging, respectively, of the meibomian glands and allow the clinician to observe the gland morphology. Atrophy of meibomian gland tissues is often termed 'meibomian gland dropout', and evaluation of these structures can inform the clinician of the severity, prognosis, and potential treatment efficacy of MGD. Gland architecture can be evaluated clinically using means that include eyelid transillumination [103], OCT [104–108], infrared video or photography [109–113], or a combination of both eyelid transillumination and infrared imaging (i.e., dynamic meibomian imaging) [113,114]. Using eyelid transillumination, meibomian gland acini appear as dark grape-like structures relative to the surrounding tissue; whereas, under infrared illumination, the acinar structures appear hyperluminescent. There is no single standard for grading loss of meibomian gland tissues, however a number of grading scales are summarised elsewhere [69,115,116].

4.3.1.2.3. Gland expression

Expression of the meibomian glands allows for examining the meibum, as a diagnostic procedure or as a therapeutic procedure for MGD. Digital expression involves using the edge of a finger to apply pressure against the eyelids [117,118]. The Meibomian Gland Evaluator is a tool that exerts a standardised pressure of 1.25 g/mm^2 over an area of 40 mm^2 distributed across approximately eight glands [119–123]; this force intends to mimic a natural blink, and is useful for diagnostic purposes. A clinician can also apply pressure to the eyelids, supported by a spatula or Mastrota paddle [123]. Application of compressive forces to the eyelids has also been described using forceps [118,122,124], cotton-tipped applicators and cotton buds [122,125].

Assessing the number of glands yielding liquid secretions allows the clinician to evaluate how many meibomian glands express meibum and the quality of the secretion. Lower counts are associated with dry eye symptoms [119], but counts have been shown to increase after MGD treatment [126–128]. To assess the number of glands yielding liquid secretions, the glands in the inferior eyelids are expressed for 10 to 15 seconds, across three zones (temporal, central, nasal). The number of glands that produce liquid secretions are counted, factoring in the quality of the secretion [119,126–128].

4.3.1.2.3.2. Meibum quality

The composition and physical properties of meibum are altered in MGD. Therefore, as part of the evaluation of meibomian gland health, meibum quality is assessed. The glands may be expressed using one of the methods described above, and the quality of the meibum (from best to worst) can take the form of clear oil, clear oil with particulates, cloudy oil, yellow/white

opaque and semi-solid paste. There are several grading methods for evaluating meibum quality, however not any single one is considered a standard [69].

4.3.1.2.3.3. Ease of expression

The ease of expressing meibum from the meibomian glands allows the clinician to subjectively evaluate the extent of orifice obstruction. Ease of expressibility is inversely proportional to the amount of pressure required to achieve meibum expression, and can be assessed using a number of methods and grading scales [129,130]

4.3.2. Function

4.3.2.1. Blinking characteristics

Blinking characteristics can be analysed using video-based recordings [131–139] or with electromyography [140,141]. Capturing blinking characteristics is typically conducted without the knowledge of the patient, to avoid conscious influence on their blinking activity. Blinking characteristics have been examined in a variety of contexts, including in different cognitive, emotional and psychological states, as well as having been investigated as a measure of fatigue or sleepiness [142]. Proper blink function is important for maintaining tear stability and ocular surface integrity.

4.3.2.1.1. Blink rate

Blink rates have shown to be increased in individuals with dry eye disease and may have an impact on visual function and quality of life [135]. After capturing video recordings, the blink rate could be obtained by manually counting the number of blinks over a set period of time. Software can be developed to automatically count blinks [143], which could be incorporated into modern clinical instruments [136,144,145].

4.3.2.1.2. Blink completeness

Incomplete blinking has been reported to be associated with a number of conditions, including exposure keratopathy, dry eye disease, increased contact lens deposition, and LWE [146,147]; it has been implicated as a possible trigger in the natural history of dry eye disease [148]. Assessing blink completeness provides information about the quality of a blink [149]. As with blink rate, the measure of blink completeness can be facilitated using software algorithms [136,137,144] and with grading scales [149].

4.3.2.1.3. Ocular Protection Index

The Ocular Protection Index (OPI) defines a ratio between the tear breakup time (TBUT) and inter-blink interval, and is a measure of how well the ocular surface is protected by a continuous tear film. In the case where TBUT is less than that of the interblink interval (OPI <

1), then the ocular surface is exposed. However, if the OPI ≥ 1, then the ocular surface is considered sufficiently protected by tears between blinks [150,151].

4.3.2.2. Assessment for eyelid dysfunction

Eyelid dysfunction, such as lagophthalmos, can cause significant ocular discomfort [152]. Lagophthalmos can be detected by patient self-report, from video-recordings of blinking, or by instilling fluorescein and examining for inferior corneal staining. The Korb-Blackie lid seal test can also be used to evaluate the degree of eye closure; it is performed by placing a transilluminator in direct contact with the closed eyelids [153]. Light emanating from between the eyelid margins indicates areas where the eyelids do not form a complete seal, and thus where the ocular surface is at risk of exposure [153].

5.3. Clinical assessment of the lacrimal system

Clinical assessment of the lacrimal system is essential to exclude ocular pathology. Clinical testing typically begins with a visual inspection of the face and periorbital region, the position and anatomy of the eyelids and punctum, and assessment for any facial asymmetry.

5.3.1. Slit lamp examination

Detailed inspection, using slit lamp biomicroscopy, can be used to detect a range of abnormalities, including entropion, trichiasis, eyelid laxity, lagophthalmos, and caruncular swelling. These, and other, conditions may interfere with the lacrimal pump mechanism and result in eye watering and epiphora. This examination should also consider any potential obstruction of the puncta, the presence of ocular surface foreign bodies, and swelling or redness of the lacrimal sac that might indicate dacryocystitis.

5.3.2. ROPLAS test

Regurgitation on pressure over the lacrimal sac (ROPLAS) is a simple clinical test that is often used as a first line test for nasolacrimal duct obstruction. It is performed by applying steady pressure on the lacrimal sac area using an index finger. Regurgitation of mucopurulent or watery discharge from the punctum indicates nasolacrimal duct obstruction or blockage, in the lower end of the lacrimal sac. This test has very high specificity (99%) indicating a positive ROPLAS test will almost always confirm a nasolacrimal duct obstruction [154].

5.3.3. Lacrimal irrigation

Lacrimal irrigation, also termed lacrimal lavage or syringing, is often considered a gold standard test for assessing nasolacrimal duct obstruction [155,156]. It can be performed with, or without, topical anaesthetic. The lacrimal puncta are gently widened using a dilating tool, and saline is injected via a lacrimal cannula. Reflux of saline through the same punctum is indicative of obstruction within the same canaliculus; reflux of saline from both puncta indicates an obstruction at the common canaliculus. Smooth passage of saline through the nose and throat indicates patency, whereas mixed results suggest partial obstruction [157].

5.3.4. Dye disappearance test

The dye disappearance test is also used for assessment of nasolacrimal duct obstruction. Fluorescein is instilled into the inferior fornix of both eyes and after five minutes the tear film and meniscus are observed under a cobalt blue light for signs of dye retention. In a healthy, patent lacrimal drainage system, the fluorescein should completely disappear. Any amount of dye remaining after five minutes suggests complete or partial duct obstruction. Any asymmetry between the eyes should also be noted [158].

5.3.5. Jones I and II test

The Jones I test examines the patency of the lacrimal drainage system by instilling fluorescein in the conjunctival sac, followed by retrieving the drained fluorescein from under the inferior turbinate (near the nasal cavity) after two to five minutes. Positive dye recovery indicates a functionally patent drainage system, although false-negative results are not uncommon, particularly in cases of partial obstruction. The Jones II test is performed if the Jones I is negative. For this test, the conjunctiva is cleared of any remaining fluorescein dye and the lacrimal drainage system is irrigated with saline. Subsequent identification of fluorescein from the nose, by placement of a cotton bud or equivalent, suggests a degree of patency, whereas fluorescein reflux indicates obstruction. These tests are performed relatively infrequently, as the procedure requires skill, and is associated with high false-positive and false-negative test outcomes [157].

5.3.6. Surgical and other procedural assessments

Several surgical and procedural tests can be used to examine the integrity of the lacrimal drainage system. Probing may be indicated if lacrimal irrigation (see Section 5.3.3 of the main CLEAR Anatomy Report) reveals a drainage obstruction [159]. Probing is generally performed by dilating the punctum after topical anaesthesia. Carefully respecting the lacrimal drainage system anatomy, an appropriately sized lacrimal probe is then passed through the punctum, and along the canaliculi, until it reaches a physical stop [160]. A ‘hard stop’ occurs when the probe makes contact with bone, and indicates patency of the individual canaliculus, the

common canaliculus, and the opening to the lacrimal sac. A ‘soft stop’, where distension of the drainage system membranes is accompanied by resistance, indicates a common canalicular or individual canalicular blockage [160].

Examination of the nasal cavity using endoscopy is indicated for patients with suspected nasolacrimal duct obstruction [161] and can identify conditions, such as a deviated nasal septum, hypertrophied turbinate or other anatomical abnormality that may require surgical intervention [162]. Similar to other endoscopies, the procedure involves using a thin, flexible tube with a tiny camera and a light to inspect any abnormality in the nasal cavity. This test provides a detailed assessment of the nasolacrimal drainage system and is often obligatory for patients being considered for lacrimal surgery [163].

For further investigation of the anatomy of the lacrimal drainage system, nasal scintillography or contrast dacryocystography can be performed [164]. This is a radiographic examination that requires administration of a contrast medium into the ducts. The flow of contrast medium from the puncta to the nasal cavity characterises the patency and anatomy of the system. A dacryocystogram of a healthy drainage system should show sequential passage of dye through the lacrimal drainage apparatus, and an absence of radiolabelled fluid would indicate a complete or partial blockage in the respective area.

6.3. Clinical assessment of the tear film

6.3.1. Clinical history and symptom assessment

An important component of clinical history taking involves enquiring about dry eye risk factors, such as medications, general health conditions, smoking and contact lens wear. Symptoms, which include discomfort and visual disturbance, are an essential part of a dry eye diagnosis [165]. For dry eye screening, the TFOS Dry Eye Workshop II (DEWS II) Diagnostic Methodology report recommends the use of the Dry Eye Questionnaire - 5 item (DEQ-5) with a cut-off value ≥6, or the Ocular Surface Disease Index (OSDI) questionnaire with a cut-off value ≥13 [4] (Figure 19). More recently, a shortened and simplified version of the OSDI, named the OSDI-6, was proposed as an alternative [166]. The Symptom Assessment in Dry Eye (SANDE) questionnaire has been tested within a rapid non-invasive battery of tests against the TFOS DEWS II criteria and found to have a sensitivity of 83% and specificity of 82% for identifying dry eye symptoms, using a cut-off score of ≥30 [167]. Dry eye symptoms are more frequent in contact lens wearers than in non-lens wearers [168,169]. To detect these symptoms in contact lens wearers validated questionnaires such as the Standard Patient

Evaluation of Eye Dryness (SPEED), the Contact Lens Dry Eye Questionnaire (CLDEQ) or the 8-Item Contact Lens Dry Eye Questionnaire-8 (CLDEQ-8) are recommended [170–172].

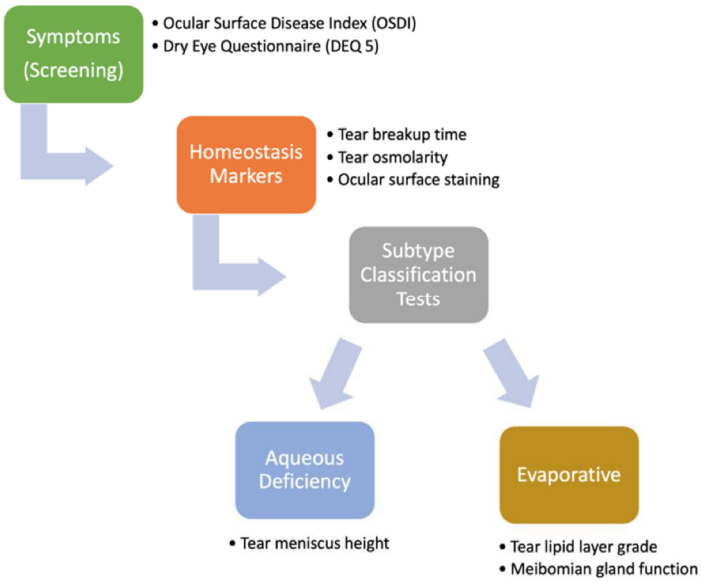

Figure 19: Summary of the clinical process for dry eye disease diagnosis and subtyping evaluation, adapted from [4].

6.3.2. Clinical assessments

6.3.2.1. Slit lamp biomicroscopy

Slit lamp examination is valuable for directly and indirectly assessing tear health. Relevant signs associated with tear dysfunction, which are identifiable on slit lamp examination, include ocular surface damage (see also Section 2.3.1.1 and Section 3.1.3.1), inadequate tear volume, reduced TBUT, conjunctival hyperaemia, blinking irregularities, and MGD. When assessing tear quality, frothing, foaming and/or debris may be indicative of blepharitis or MGD [69]. Slit lamp examination can be used to quantify ocular surface damage, as an indirect measure of tear quality, through quantifying signs such as corneal and conjunctival staining patterns (see Section 2.3.1 and Section 3.1.3 of the main CLEAR Anatomy Report, respectively) and LIPCOF (see Section 3.1.3.1 of the main CLEAR Anatomy Report).

6.3.2.2. Tear osmolarity

Tear osmolarity, as a marker of tear homeostasis, is an important factor in dry eye disease [173]. Elevated tear osmolarity (tear hyperosmolarity) signifies tear imbalance. Clinical assessment of tear osmolarity is a key component of the TFOS DEWS II diagnostic methodology report [4].

Traditional methods for measuring tear osmolarity include freezing point depression [174] and vapour pressure osmometry [175]; both are laboratory-based techniques that are hampered

by the necessarily small volumes of tear samples. Point-of-care systems that use electrical impedance to rapidly measure the osmolarity are now available [176]. One such system has been validated against established techniques [177], although measurement reliability has been debated [178,179].

While assessing variations in osmolarity across the tear film surface would be desirable [180–182], practical and methodological constraints have generally limited the site of measurement to the lower tear meniscus. Gad et al. described a protocol for measuring tear osmolarity at the superior and inferior lateral menisci, a parameter defined as the Inferior-Superior Osmotic Difference (I-SOD), and reported higher levels of asymmetry between these two measures in individuals with contact lens discomfort [183]. For diagnosing dry eye disease, the TFOS DEWS II protocol recommends a criterion, based on the TearLab™ system (TearLab Corporation, US, being the one available at the time), of ≥ 308 mOsm/L in either eye, or an interocular difference of > 8 mOsm/L [4]. Individuals with more severe dry eye generally have higher absolute levels of tear osmolarity and increased inter-eye variability over time [184–186].

6.3.2.3. Tear stability

Maintaining tear film integrity is critical for ocular surface health, to avoid desiccation. The length of time that the tears remain intact, as a film over the eye's surface, after a blink is described as the TBUT. Tear film instability is a key pathophysiological feature of dry eye disease [173,187], and (in addition to tear osmolarity) a sign of homeostatic imbalance, according to the TFOS DEWS II criteria [4].

6.3.2.3.1. Fluorescein tear breakup time

TBUT is commonly measured after instillation of fluorescein into the eye [188–190]; this procedure enhances visibility of the tear film using slit lamp observation with a blue light, and can be further optimised with use of a yellow barrier filter [13]. TBUT is recorded as the time between a complete blink and the appearance of a dark streak, or patch, in the tear film layer; a value of <10 seconds is generally regarded as abnormal [191]. Fluorescein TBUT has a number of limitations; however, the most significant is disruption to the tear film [192], due to the volume and pH of the instilled fluid, which fundamentally affects the parameter the test intends to measure [193–195]. The accuracy of fluorescein TBUT measures can be improved by minimising the volume of fluid instilled [192].

6.3.2.3.2. Non-invasive tear break-up time

Tear stability assessment methods that avoid tear film disruption are preferred over invasive techniques; non-invasive tear breakup time (NIBUT) measurements are thus recommended, wherever possible[4]. For NIBUT measurements, a patterned grid or videokeratoscope mires

are reflected from the tear film surface (Figure 20), and observed after a blink for the first sign of distortion or disruption of the pattern [196,197]. NIBUT can be assessed subjectively, using a stopwatch to record the time to tear breakup, or objectively with diagnostic instrumentation that offers automated NIBUT detection [198]. With any tear film stability measurement technique, an average of three values should be recorded. While some variation in optimal technique and instrument-specific cut-offs has been reported and ethnic variations in tear film stability are recognised [199]; currently, a NIBUT of <10 seconds is used to signify homeostatic imbalance according to the TFOS DEWS II diagnostic criteria [4]. Measures of fluorescein TBUT and NIBUT are not interchangeable, and a consistent approach is preferable for the longitudinal evaluation of patients [193–195].

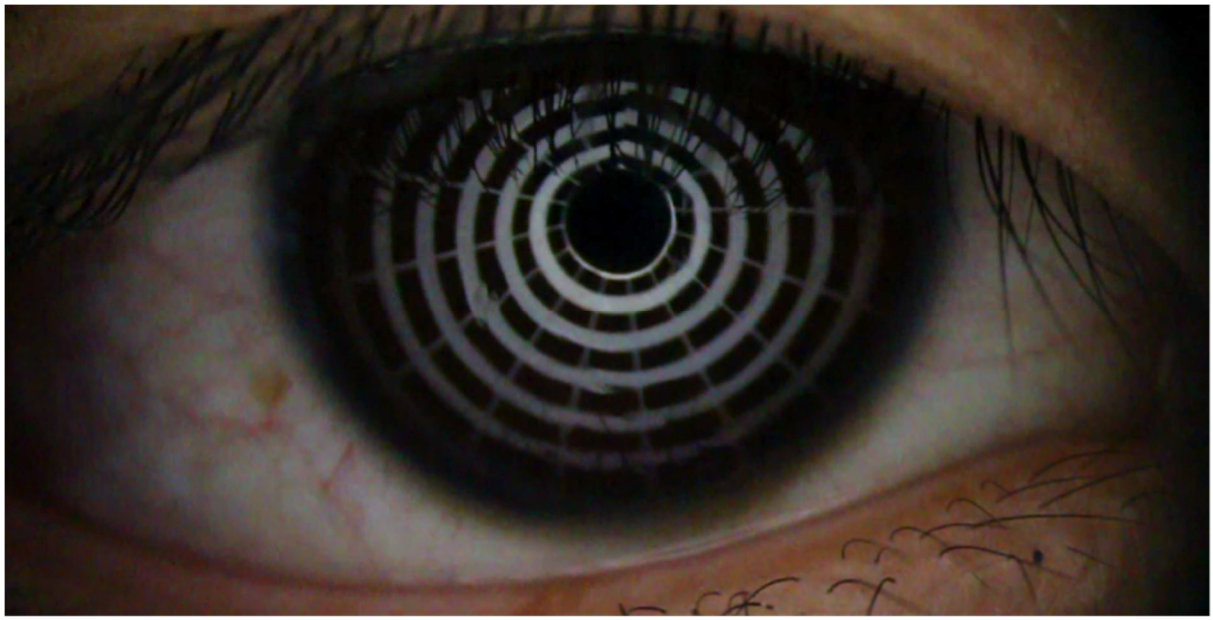

Figure 20: Placido disc mires reflected from the tear film surface. Distortions in the reflected mire pattern visible at 6 o'clock and 8 o'clock positions, signifying non-invasive tear film breakup.

6.3.2.4. Lipid layer evaluation

An intact tear lipid layer is critical to inhibit tear evaporation. Thinner tear lipid layers are associated with poorer tear stability than thicker layers [200]. Given that meibum comprises a major part of tear lipids, evaluation of the tear lipid layer can provide insight into meibomian gland function. The higher refractive index of the thin tear lipid layer, relative to the underlying muco-aqueous phase, lends itself to evaluation by thin film interferometry (Figure 21). Broad spectrum, wide-field illumination of the lipid layer highlights interference fringe patterns that can be graded to reflect the estimated lipid layer thickness and integrity [102,201,202]. In increasing order of thickness, intact lipid layer patterns are described as open meshwork

(grade 1), closed meshwork (grade 2), wave (grade 3) (Figure 21), amorphous (grade 4) and colour fringe (grade 5). Clinically non-visible lipid patterns, or abnormal colour fringe patterns that signify clumps of lipid floating amidst areas of little or no lipid cover, do not inhibit tear evaporation [200], and as such are considered non-functional (grade 0). Lipid layer grade has been shown to be a discriminative marker for evaporative dry eye disease [203].

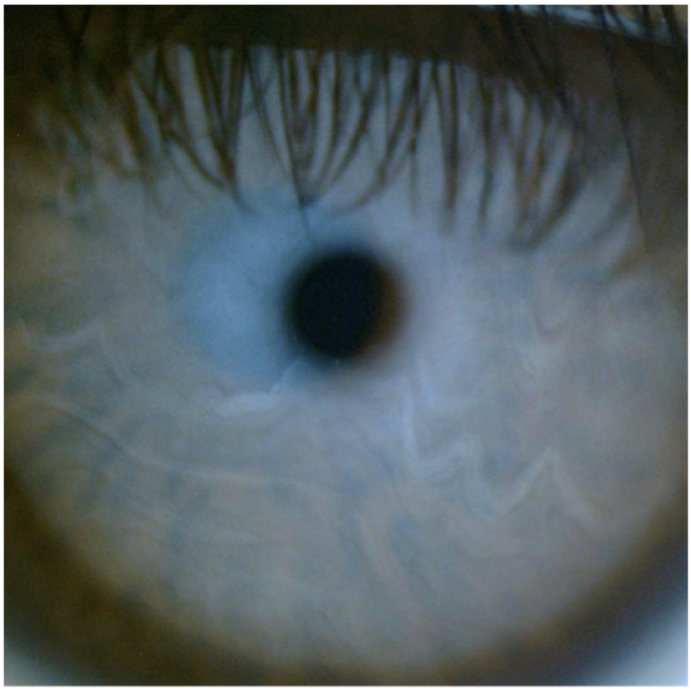

Figure 21: Wave lipid pattern (equating to grade 3 on the modified Guillon scale) [102,201,202] viewed interferometrically using a wide-field, cold light source.

A slit lamp-mounted cold light tube was the earliest clinical approach for subjectively grading tear lipid layer patterns [201]. Many other devices are now available, some of which offer automated estimates of lipid layer grade [204,205]. Videokeratoscopic devices can also permit subjective interferometric evaluation of the lipid layer [205].

6.3.2.5. Tear volume

On the eye, tear fluid resides in the exposed area between the inferior and superior eyelids, conjunctival sacs and tear menisci along the eyelid margins. The total volume of tear fluid on the normal eye is estimated to be about 7 to 9 µl, with an average turnover rate of 11 to 30% per minute [206–209].

6.3.2.5.1. Schirmer test (I, II) and Phenol red thread

The two traditional tests used to evaluate tear production are the Schirmer test and Phenol red thread test [210,211]. While in the Schirmer test I the end of a 35 mm long and 5 mm wide strip of filter paper is inserted for 5 minutes into the temporal part of the lower conjunctival sac, the Phenol red thread test uses a fine cotton thread that is left in the same place for 15 seconds

[210,212]. If there is less than 10mm wetting an aqueous deficient dry eye is assumed [213,214]. Both tests are relatively invasive and poorly repeatable, even with the application of topical anaesthesia, and are influenced by reflex tear production induced by stimulation during testing [4,210,215]. The Schirmer II test describes the test conducted with intranasal stimulation with a cotton tip applicator. For the Schirmer test, a cut off value of 5 mm is generally considered indicative of a dry eye [216].

6.3.2.5.2. Tear meniscus evaluation

About 75% to 90% of the on-eye tear volume lies in the menisci [217–219]. Evaluation of the tear meniscus at the midpoint of the eyelid is used as an indicator of tear volume [220,221]. Different parameters have been used to describe the tear meniscus, including features such as tear meniscus height (TMH), radius, depth and cross-sectional area [56,222–224]. Various quantification methods have been used (Figure 22A), including slit lamp evaluation (with or without associated image capture), reflective meniscometry, interferometry and OCT (Figure 22B) [225–228]. Recent advances allow automatic tear meniscus measurement and tear volume analysis [228,229]. Depending on the technique used, TMH in healthy eyes varies between 0.12 and 0.46 mm [223,230,231]. A TMH criterion of <0.2 mm has been suggested to be diagnostic for aqueous deficiency [4]. Tear meniscus parameters can be influenced by time after blink, diurnal variations, measurement location along the eyelids, presence of LIPCOF (see Section 3.1.3.1), climate and illumination technique [4,232–235].

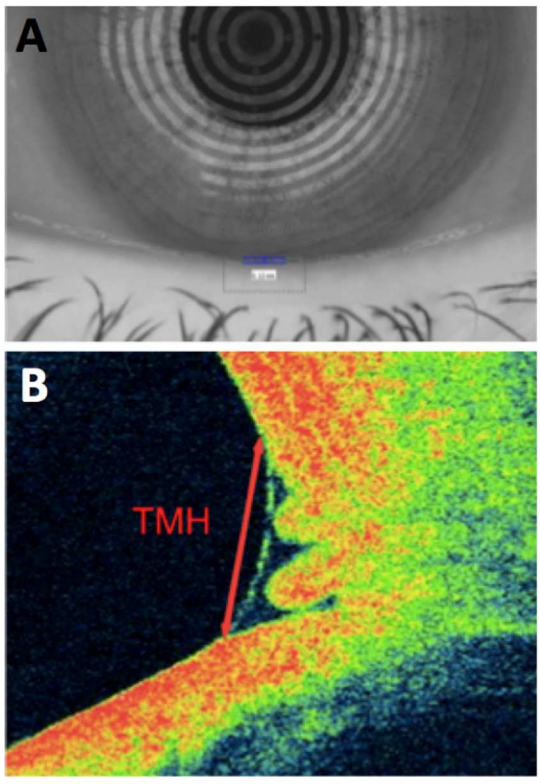

Figure 22. A: Tear meniscus height (TMH) measured with the image capture module of the Keratograph 5M. B. TMH measured on an OCT image, with lid parallel conjunctival folds (LIPCOF grade 2) protruding into the meniscus [56].

6.3.2.5.3. Tear clearance

Tear turnover rate, defined as the rate of change in tear volume over a set time period, can be measured clinically by assessing the percentage decrease of fluorescein concentration in the tears per minute [207]. In the fluorescein clearance test, a standardised amount and concentration of fluorescein is instilled into the inferior conjunctival sac. The remaining fluorescein concentration after a specific time can be measured with a fluorometer or a visual grading scale [236–238]. More recently, OCT was used for evaluation of early-phase tear clearance without fluorescein [239,240].

6.3.2.6. Other

A range of other methods (e.g. tear film ferning, visual disturbance tests, ocular surface sensitivity, thermography) have been investigated for direct and indirect tear film assessment; these methods have been summarised in detail elsewhere [4].

References

[1] Wolffsohn JS, Dumbleton K, Huntjens B, Kandel H, Koh S, Kunnen CME, et al. CLEAR - evidence based contact lens practice. Cont Lens Anterior Eye 2021;44:In press.

[2] Martin R. Cornea and anterior eye assessment with slit lamp biomicroscopy, specular microscopy, confocal microscopy, and ultrasound biomicroscopy. Indian J Ophthalmol 2018;66:195–201.

[3] Begley C, Caffery B, Chalmers R, Situ P, Simpson T, Nelson JD. Review and analysis of grading scales for ocular surface staining. Ocul Surf 2019;17:208–20.

[4] Wolffsohn JS, Arita R, Chalmers R, Djalilian A, Dogru M, Dumbleton K, et al. TFOS DEWS II Diagnostic Methodology report. Ocul Surf 2017;15:539–74.

[5] Lemp MA. Report of the National Eye Institute/Industry workshop on Clinical Trials in Dry Eyes. CLAO J 1995;21:221–32.

[6] Bron AJ, Evans VE, Smith JA. Grading of corneal and conjunctival staining in the context of other dry eye tests. Cornea 2003;22:640–50.

[7] Caffery BE, Josephson JE. Corneal staining after sequential instillations of fluorescein over 30 days. Optom Vis Sci 1991;68:467–9.

[8] Abelson MB, Farvo DWR, Shapiro A, Ousler G III. Diagnosing dry eye: It's now a fine art. Ophthalmol Manag 2016;20:48–50.

[9] Bron AJ, Argüeso P, Irkec M, Bright FV. Clinical staining of the ocular surface: mechanisms and interpretations. Prog Retin Eye Res 2015;44:36–61.

[10] van Bijsterveld OP. Diagnostic Tests in the Sicca Syndrome. Arch Ophthalmol 1969;82:10–4.

[11] Terry RL, Schnider CM, Holden BA, Cornish R, Grant T, Sweeney D, et al. CCLRU standards for success of daily and extended wear contact lenses. Optom Vis Sci 1993;70:234–43.

[12] Efron N, Morgan PB, Katsara SS. Validation of grading scales for contact lens complications. Ophthalmic Physiol Opt 2001;21:17–29.

[13] Peterson RC, Wolffsohn JS, Fowler CW. Optimization of anterior eye fluorescein viewing. Am J Ophthalmol 2006;142:572–5.

[14] Efron N, Jones L, Bron AJ, Knop E, Arita R, Barabino S, et al. The TFOS International Workshop on Contact Lens Discomfort: report of the contact lens interactions with the ocular surface and adnexa subcommittee. Invest Ophthalmol Vis Sci 2013;54:TFOS98–122.

[15] Chan CC, Holland EJ. Severe limbal stem cell deficiency from contact lens wear: patient clinical features. Am J Ophthalmol 2013;155:544–9.e2.

[16] Martin R. Corneal conjunctivalization management with high Dk RGP contact lenses. Cont Lens Anterior Eye 2009;32:147–50.

[17] Rossen J, Amram A, Milani B, Park D, Harthan J, Joslin C, et al. Contact Lens-induced Limbal Stem Cell Deficiency. Ocul Surf 2016;14:419–34.

[18] Stapleton F, Bakkar M, Carnt N, Chalmers R, Kumar A, Marasini S, et al. CLEAR - contact lens complications. Cont Lens Anterior Eye 2021;44:In press.

[19] Jiao H, Hill LJ, Downie LE, Chinnery HR. Anterior segment optical coherence tomography: its application in clinical practice and experimental models of disease. Clin Exp Optom 2019;102:208–17.

[20] Fan R, Chan TC, Prakash G, Jhanji V. Applications of corneal topography and tomography: a review. Clin Experiment Ophthalmol 2018;46:133–46.

[21] Courville CB, Smolek MK, Klyce SD. Contribution of the ocular surface to visual optics. Exp Eye Res 2004;78:417–25.

[22] Iskander DR, Wachel P, Simpson PND, Consejo A, Jesus DA. Principles of operation, accuracy and precision of an Eye Surface Profiler. Ophthalmic Physiol Opt 2016;36:266–78.

[23] Drexler W, Morgner U, Ghanta RK, Kärtner FX, Schuman JS, Fujimoto JG. Ultrahigh-resolution ophthalmic optical coherence tomography. Nat Med 2001;7:502–7.
[24] Vincent SJ, Alonso-Caneiro D, Collins MJ. Optical coherence tomography and scleral contact lenses: clinical and research applications. Clin Exp Optom 2019;102:224–41.
[25] Fuentes E, Sandali O, El Sanharawi M, Basli E, Hamiche T, Goemaere I, et al. Anatomic Predictive Factors of Acute Corneal Hydrops in Keratoconus: An Optical Coherence Tomography Study. Ophthalmology 2015;122:1653–9.
[26] Vajzovic LM, Karp CL, Haft P, Shousha MA, Dubovy SR, Hurmeric V, et al. Ultra high-resolution anterior segment optical coherence tomography in the evaluation of anterior corneal dystrophies and degenerations. Ophthalmology 2011;118:1291–6.
[27] Yenerel NM, Kucumen RB, Gorgun E. The complementary benefit of anterior segment optical coherence tomography in penetrating keratoplasty. Clin Ophthalmol 2013;7:1515–23.
[28] Shousha MA, Karp CL, Perez VL, Hoffmann R, Ventura R, Chang V, et al. Diagnosis and management of conjunctival and corneal intraepithelial neoplasia using ultra high-resolution optical coherence tomography. Ophthalmology 2011;118:1531–7.
[29] Deinema LA, Vingrys AJ, Chinnery HR, Downie LE. Optical Coherence Tomography Reveals Changes to Corneal Reflectivity and Thickness in Individuals with Tear Hyperosmolarity. Transl Vis Sci Technol 2017;6:6.
[30] Minsky M. Memoir on inventing the confocal scanning microscope. Scanning 1988;10:128–38.
[31] Chinnery HR, Naranjo Golborne C, Downie LE. Omega-3 supplementation is neuroprotective to corneal nerves in dry eye disease: a pilot study. Ophthalmic Physiol Opt 2017;37:473–81.
[32] Jonuscheit S, Doughty MJ, Ramaesh K. In vivo confocal microscopy of the corneal endothelium: comparison of three morphometry methods after corneal transplantation. Eye 2011;25:1130–7.
[33] Cruzat A, Qazi Y, Hamrah P. In Vivo Confocal Microscopy of Corneal Nerves in Health and Disease. Ocul Surf 2017;15:15–47.
[34] Bitirgen G, Ozkagnici A, Malik RA, Oltulu R. Evaluation of Contact Lens–Induced Changes in Keratoconic Corneas Using In Vivo Confocal Microscopy. Invest Ophthalmol Vis Sci 2013;54:5385–91.
[35] Mastropasqua L, Nubile M, Lanzini M, Carpineto P, Ciancaglini M, Pannellini T, et al. Epithelial dendritic cell distribution in normal and inflamed human cornea: in vivo confocal microscopy study. Am J Ophthalmol 2006;142:736–44.
[36] Chidambaram JD, Prajna NV, Larke NL, Palepu S, Lanjewar S, Shah M, et al. Prospective Study of the Diagnostic Accuracy of the In Vivo Laser Scanning Confocal Microscope for Severe Microbial Keratitis. Ophthalmology 2016;123:2285–93.
[37] Hau SC, Dart JKG, Vesaluoma M, Parmar DN, Claerhout I, Bibi K, et al. Diagnostic accuracy of microbial keratitis with in vivo scanning laser confocal microscopy. Br J Ophthalmol 2010;94:982–7.
[38] Stave J, Zinser G, Grümmer G, Guthoff R. Modified Heidelberg Retinal Tomograph HRT. Initial results of in vivo presentation of corneal structures. Ophthalmologe 2002;99:276–80.
[39] Zhivov A, Stachs O, Kraak R, Stave J, Guthoff RF. In vivo confocal microscopy of the ocular surface. Ocul Surf 2006;4:81–93.
[40] De Silva MEH, Zhang AC, Karahalios A, Chinnery HR, Downie LE. Laser scanning in vivo confocal microscopy (IVCM) for evaluating human corneal sub-basal nerve plexus parameters: protocol for a systematic review. BMJ Open 2017;7:e018646.
[41] Connor CG, Zagrod ME. Contact lens-induced corneal endothelial polymegathism: functional significance and possible mechanisms. Am J Optom Physiol Opt 1986;63:539–44.
[42] Barnett M, Courey C, Fadel D, Lee K, Michaud L, Montani G, et al. CLEAR scleral lenses. Cont Lens Anterior Eye 2021;44:In press.

[43] Efron N. Efron Grading Scales for Contact Lens Complications (Millennium Edition), Butterworth-Heinemann 2000.
[44] Efron N. Clinical application of grading scales for contact lens complications. Optician 1997;213:26–34.
[45] Lofstrom T, Anderson JS, Kruse A. Tarsal abnormalities: a new grading system. CLAO J 1998;24:210–5.
[46] Phillips AJ, Speedwell L, Makepeace C. CCLRU grading scales (Appendix D). Contact Lenses 1997:863–7.
[47] Downie LE, Keller PR, Vingrys AJ. Assessing ocular bulbar redness: a comparison of methods. Ophthalmic Physiol Opt 2016;36:132–9.
[48] Höh H, Schirra F, Kienecker C, Ruprecht KW. Lid-parallel conjunctival folds are a sure diagnostic sign of dry eye. Ophthalmologe 1995;92:802–8.
[49] Pult H, Tosatti SGP, Spencer ND, Asfour J-M, Ebenhoch M, Murphy PJ. Spontaneous Blinking from a Tribological Viewpoint. Ocul Surf 2015;13:236–49.
[50] Berry M, Pult H, Purslow C, Murphy PJ. Mucins and ocular signs in symptomatic and asymptomatic contact lens wear. Optom Vis Sci 2008;85:E930–8.
[51] Pult H, Riede-Pult BH, Murphy PJ. The relation between blinking and conjunctival folds and dry eye symptoms. Optom Vis Sci 2013;90:1034–9.
[52] Pult H, Bandlitz S. Lid-Parallel Conjunctival Folds and Their Ability to Predict Dry Eye. Eye Contact Lens 2018;44 Suppl 2:S113–9.
[53] Németh J, Fodor E, Lang Z, Kosina-Hagyó K, Berta A, Komár T, et al. Lid-parallel conjunctival folds (LIPCOF) and dry eye: a multicentre study. Br J Ophthalmol 2012;96:1380–5.
[54] Pult H, Murphy PJ, Purslow C. A novel method to predict the dry eye symptoms in new contact lens wearers. Optom Vis Sci 2009;86:E1042–50.
[55] Veres A, Tapasztó B, Kosina-Hagyó K, Somfai GM, Németh J. Imaging lid-parallel conjunctival folds with OCT and comparing its grading with the slit lamp classification in dry eye patients and normal subjects. Invest Ophthalmol Vis Sci 2011;52:2945–51.
[56] Bandlitz S, Purslow C, Murphy PJ, Pult H. Influence of Conjunctival Folds on Calculated Tear Meniscus Volume Along the Lower Eyelid. Ocul Surf 2016;14:377–84.
[57] Bandlitz S, Purslow C, Murphy PJ, Pult H. The relationship between tear meniscus regularity and conjunctival folds. Optom Vis Sci 2014;91:1037–44.
[58] Korb DR, Herman JP, Finnemore VM, Exford JM, Blackie CA. An evaluation of the efficacy of fluorescein, rose bengal, lissamine green, and a new dye mixture for ocular surface staining. Eye Contact Lens 2008;34:61–4.
[59] Tseng SC, Feenstra RP, Watson BD. Characterization of photodynamic actions of rose bengal on cultured cells. Invest Ophthalmol Vis Sci 1994;35:3295–307.
[60] Hamrah P, Alipour F, Jiang S, Sohn J-H, Foulks GN. Optimizing evaluation of Lissamine Green parameters for ocular surface staining. Eye 2011;25:1429–34.
[61] Toda I, Tsubota K. Practical double vital staining for ocular surface evaluation. Cornea 1993;12:366–7.
[62] Awisi Gyau D, Begley CG, Daniel Nelson J. A simple and cost effective method for preparing FL and LG solutions. Ocul Surf 2018;16:139–45.
[63] Chan TCY, Ye C, Ng PKF, Li EYM, Yuen HKL, Jhanji V. Change in Tear Film Lipid Layer Thickness, Corneal Thickness, Volume and Topography after Superficial Cauterization for Conjunctivochalasis. Sci Rep 2015;5:12239.
[64] Whitcher JP, Shiboski CH, Shiboski SC, Heidenreich AM, Kitagawa K, Zhang S, et al. A simplified quantitative method for assessing keratoconjunctivitis sicca from the Sjögren's Syndrome International Registry. Am J Ophthalmol 2010;149:405–15.
[65] Chang SW, Hou PK, Chen MS. Conjunctival concretions. Polarized microscopic, histopathologic, and ultrastructural studies. Arch Ophthalmol 1990;108:405–7.
[66] Bron AJ, Benjamin L, Snibson GR. Meibomian gland disease. Classification and grading of lid changes. Eye 1991;5 (Pt 4):395–411.
[67] Foulks GN, Bron AJ. Meibomian gland dysfunction: a clinical scheme for description, diagnosis, classification, and grading. Ocul Surf 2003;1:107–26.

[68] Hykin PG, Bron AJ. Age-related morphological changes in lid margin and meibomian gland anatomy. Cornea 1992;11:334–42.
[69] Tomlinson A, Bron AJ, Korb DR, Amano S, Paugh JR, Pearce EI, et al. The international workshop on meibomian gland dysfunction: report of the diagnosis subcommittee. Invest Ophthalmol Vis Sci 2011;52:2006–49.
[70] Amador GJ, Mao W, DeMercurio P, Montero C, Clewis J, Alexeev A, et al. Eyelashes divert airflow to protect the eye. J R Soc Interface 2015;12. https://doi.org/10.1098/rsif.2014.1294.
[71] Patel BC, Joos ZP. Diseases of the Eyelashes. StatPearls, Treasure Island (FL): StatPearls Publishing; 2019.
[72] Kumar A, Karthikeyan K. Madarosis: a marker of many maladies. Int J Trichology 2012;4:3–18.
[73] Anwar S, Jafferany M. Trichotillomania: a psychopathological perspective and the psychiatric comorbidity of hair pulling. Acta Dermatovenerol Alp Pannonica Adriat 2019;28:33–6.
[74] Modjtahedi BS, Kishan AU, Schwab IR, Jackson WB, Maibach HI. Eyelash alopecia areata: case series and literature review. Can J Ophthalmol 2012;47:333–8.
[75] Morris CL, Stinnett S, Woodward J. The role of bimatoprost eyelash gel in chemotherapy-induced madarosis: an analysis of efficacy and safety. Int J Trichology 2011;3:84–91.
[76] Smolin G, Okumoto M. Staphylococcal Blepharitis. Archives of Ophthalmology 1977;95:812–6. https://doi.org/10.1001/archopht.1977.04450050090009.
[77] Lindsley K, Matsumura S, Hatef E, Akpek EK. Interventions for chronic blepharitis. Cochrane Database Syst Rev 2012:CD005556.
[78] Fromstein SR, Harthan JS, Patel J, Opitz DL. Demodex blepharitis: clinical perspectives. Clinical Optometry 2018;10:57–63. https://doi.org/10.2147/opto.s142708.
[79] Zhang AC, Muntz A, Wang MTM, Craig JP, Downie LE. Ocular Demodex: a systematic review of the clinical literature. Ophthalmic Physiol Opt 2020;40:389–432.
[80] Wu N, Zhang H, Sun FY. Phthiriasis palpebrarum: A case of eyelash infestation with Pthirus pubis. Experimental and Therapeutic Medicine 2017;13:2000–2. https://doi.org/10.3892/etm.2017.4187.
[81] Kunnen C, Heunen M, Mertz C, Chalmers R, Soeters N, Study group. Comparison of white and blue light assessment of the upper and lower palpebral conjunctiva. Cont Lens Anterior Eye 2018;41:473–81.
[82] Doughty MJ, Potvin R, Pritchard N, Fonn D. Evaluation of the range of areas of the fluorescein staining patterns of the tarsal conjunctiva in man. Doc Ophthalmol 1995;89:355–71.
[83] MacKinven J, McGuinness CL, Pascal E, Woods RL. Clinical grading of the upper palpebral conjunctiva of non-contact lens wearers. Optom Vis Sci 2001;78:13–8.
[84] Wolffsohn JS, Naroo SA, Christie C, Morris J, Conway R, Maldonado-Codina C, et al. Anterior eye health recording. Cont Lens Anterior Eye 2015;38:266–71.
[85] Korb DR, Greiner JV, Herman JP, Hebert E, Finnemore VM, Exford JM, et al. Lid-wiper epitheliopathy and dry-eye symptoms in contact lens wearers. CLAO J 2002;28:211–6.
[86] Morgan P, Murphy PJ, Gifford K, Gifford P, Golebiowski B, Johnson L, et al. CLEAR - Effect of contact lens materials and designs on the anatomy and physiology of the eye. Cont Lens Anterior Eye 2021;44:In press.
[87] Efron N, Brennan NA, Morgan PB, Wilson T. Lid wiper epitheliopathy. Prog Retin Eye Res 2016;53:140–74.
[88] Korb DR, Herman JP, Greiner JV, Scaffidi RC, Finnemore VM, Exford JM, et al. Lid wiper epitheliopathy and dry eye symptoms. Eye Contact Lens 2005;31:2–8.
[89] Varikooty J, Srinivasan S, Subbaraman L, Woods CA, Fonn D, Simpson TL, et al. Variations in observable lid wiper epitheliopathy (LWE) staining patterns in wearers of silicone hydrogel lenses. Cont Lens Anterior Eye 2015;38:471–6.

[90] Moezzi AM, Varikooty J, Luensmann D, Schulze M-M, Ng A, Karkkainen T, et al. The short-term physiological impact of switching reusable silicone hydrogel wearers into a hydrogel daily disposable multifocal. Clin Ophthalmol 2019;13:1193–202.
[91] Li W, Yeh TN, Leung T, Yuen T, Lerma M, Lin MC. The Relationship of Lid Wiper Epitheliopathy to Ocular Surface Signs and Symptoms. Invest Ophthalmol Vis Sci 2018;59:1878–87.
[92] Lievens CW, Norgett Y, Briggs N, Allen PM, Vianya-Estopa M. Optimal methodology for lid wiper epitheliopathy identification. Cont Lens Anterior Eye 2020. https://doi.org/10.1016/j.clae.2020.04.016.
[93] Pult H, Purslow C, Berry M, Murphy PJ. Clinical tests for successful contact lens wear: relationship and predictive potential. Optom Vis Sci 2008;85:E924–9.
[94] Schulze M-M, Srinivasan S, Hickson-Curran SB, Toubouti Y, Coz S, Mirza A, et al. Comparisons between age, gender, lens type and lid wiper epitheliopathy with soft contact lens comfort. Invest Ophthalmol Vis Sci 2015;56.
[95] Read M, Maldonado-Codina C, Morgan PB, Smith S. Development of an imaging system to detect changes in redness of the eyelid margin. Optom Vis Sci 2014;90.
[96] Yamaguchi M, Kutsuna M, Uno T, Zheng X, Kodama T, Ohashi Y. Marx line: fluorescein staining line on the inner lid as indicator of meibomian gland function. Am J Ophthalmol 2006;141:669–75.
[97] Doughty MJ, Naase T, Donald C, Hamilton L, Button NF. Visualisation of “Marx”s line’ along the marginal eyelid conjunctiva of human subjects with lissamine green dye. Ophthalmic and Physiological Optics 2004;24:1–7. https://doi.org/10.1046/j.1475-1313.2003.00160.x.
[98] Korb DR, Blackie CA. Debridement-scaling: a new procedure that increases Meibomian gland function and reduces dry eye symptoms. Cornea 2013;32:1554–7.
[99] Ngo W, Caffery B, Srinivasan S, Jones LW. Effect of Lid Debridement-Scaling in Sjögren Syndrome Dry Eye. Optom Vis Sci 2015;92:e316–20.
[100] Doughty MJ. Morphological features of cells along Marx’s line of the marginal conjunctiva of the human eyelid. Clinical and Experimental Optometry 2013;96:76–84. https://doi.org/10.1111/j.1444-0938.2012.00763.x.
[101] Norn M. Meibomian orifices and Marx’s line Studied by Triple Vital Staining. Acta Ophthalmologica 2009;63:698–700. https://doi.org/10.1111/j.1755-3768.1985.tb01584.x.
[102] Downie LE, Craig JP. Tear film evaluation and management in soft contact lens wear: a systematic approach. Clin Exp Optom 2017;100:438–58.
[103] Robin JB, Jester JV, Nobe J, Nicolaides N, Smith RE. In vivo transillumination biomicroscopy and photography of meibomian gland dysfunction. A clinical study. Ophthalmology 1985;92:1423–6.
[104] Liang Q, Pan Z, Zhou M, Zhang Y, Wang N, Li B, et al. Evaluation of Optical Coherence Tomography Meibography in Patients With Obstructive Meibomian Gland Dysfunction. Cornea 2015;34:1193–9.
[105] Hwang HS, Park CW, Joo C-K. Novel noncontact meibography with anterior segment optical coherence tomography: Hosik meibography. Cornea 2013;32:40–3.
[106] Hwang HS, Shin JG, Lee BH, Eom TJ, Joo C-K. In Vivo 3D Meibography of the Human Eyelid Using Real Time Imaging Fourier-Domain OCT. PLoS One 2013;8:e67143.
[107] Yoo Y-S, Na K-S, Byun Y-S, Shin JG, Lee BH, Yoon G, et al. Examination of Gland Dropout Detected on Infrared Meibography by Using Optical Coherence Tomography Meibography. Ocul Surf 2017;15:130–8.e1.
[108] Ju MJ, Shin JG, Hoshi S, Yasuno Y, Lee BH, Tang S, et al. Three-dimensional volumetric human meibomian gland investigation using polarization-sensitive optical coherence tomography. J Biomed Opt 2014;19:30503.
[109] Arita R, Itoh K, Inoue K, Amano S. Noncontact Infrared Meibography to Document Age-Related Changes of the Meibomian Glands in a Normal Population. Ophthalmology 2008;115:911–5. https://doi.org/10.1016/j.ophtha.2007.06.031.

[110] Arita R, Itoh K, Inoue K, Kuchiba A, Yamaguchi T, Amano S. Contact lens wear is associated with decrease of meibomian glands. Ophthalmology 2009;116:379–84.
[111] Pondelis N, Dieckmann GM, Jamali A, Kataguiri P, Senchyna M, Hamrah P. Infrared meibography allows detection of dimensional changes in meibomian glands following intranasal neurostimulation. Ocul Surf 2020. https://doi.org/10.1016/j.jtos.2020.03.003.
[112] Maskin SL, Testa WR. Infrared Video Meibography of Lower Lid Meibomian Glands Shows Easily Distorted Glands: Implications for Longitudinal Assessment of Atrophy or Growth Using Lower Lid Meibography. Cornea 2018;37:1279–86.
[113] Wong S, Srinivasan S, Murphy PJ, Jones L. Comparison of meibomian gland dropout using two infrared imaging devices. Cont Lens Anterior Eye 2019;42:311–7.
[114] Blackie CA, Coleman CA, Nichols KK, Jones L, Chen PQ, Melton R, et al. A single vectored thermal pulsation treatment for meibomian gland dysfunction increases mean comfortable contact lens wearing time by approximately 4 hours per day. Clin Ophthalmol 2018;12:169–83.
[115] Pult H, Nichols JJ. A review of meibography. Optom Vis Sci 2012;89:E760–9.
[116] Ngo W, Srinivasan S, Jones L. Historical overview of imaging the meibomian glands. Journal of Optometry 2013;6:1–8. https://doi.org/10.1016/j.optom.2012.10.001.
[117] Haworth KM, Nichols JJ, Thangavelu M, Sinnott LT, Nichols KK. Examination of human meibum collection and extraction techniques. Optom Vis Sci 2011;88:525–33.
[118] Aketa N, Shinzawa M, Kawashima M, Dogru M, Okamoto S, Tsubota K, et al. Efficacy of Plate Expression of Meibum on Tear Function and Ocular Surface Findings in Meibomian Gland Disease. Eye Contact Lens 2019;45:19–22.
[119] Korb DR, Blackie CA. Meibomian gland diagnostic expressibility: correlation with dry eye symptoms and gland location. Cornea 2008;27:1142–7.
[120] Cochener B, Cassan A, Omiel L. Prevalence of meibomian gland dysfunction at the time of cataract surgery. J Cataract Refract Surg 2018;44:144–8.
[121] Greiner JV. A single LipiFlow® Thermal Pulsation System treatment improves meibomian gland function and reduces dry eye symptoms for 9 months. Curr Eye Res 2012;37:272–8.
[122] Kunnen CME, Brown SHJ, Lazon de la Jara P, Holden BA, Blanksby SJ, Mitchell TW, et al. Influence of Meibomian Gland Expression Methods on Human Lipid Analysis Results. Ocul Surf 2016;14:49–55.
[123] Opitz D, Harthan J, Fromstein S, Hauswirth S. Diagnosis and management of meibomian gland dysfunction: optometrists' perspective. Clinical Optometry 2015:59. https://doi.org/10.2147/opto.s63484.
[124] Lee H, Kim M, Park SY, Kim EK, Seo KY, Kim T-I. Mechanical meibomian gland squeezing combined with eyelid scrubs and warm compresses for the treatment of meibomian gland dysfunction. Clin Exp Optom 2017;100:598–602.
[125] Toyos R, Toyos M, Willcox J, Mulliniks H, Hoover J. Evaluation of the Safety and Efficacy of Intense Pulsed Light Treatment with Meibomian Gland Expression of the Upper Eyelids for Dry Eye Disease. Photobiomodul Photomed Laser Surg 2019;37:527–31.
[126] Nowinska AK, Módis L, Koprowski R, Merayo-Lloves J. Novel Diagnostic and Therapeutic Methods in Ocular Surface and Corneal Diseases. J Ophthalmol 2017;2017:6137821.
[127] Hagen KB, Bedi R, Blackie CA, Christenson-Akagi KJ. Comparison of a single-dose vectored thermal pulsation procedure with a 3-month course of daily oral doxycycline for moderate-to-severe meibomian gland dysfunction. Clin Ophthalmol 2018;12:161–8.
[128] Lane SS, DuBiner HB, Epstein RJ, Ernest PH, Greiner JV, Hardten DR, et al. A new system, the LipiFlow, for the treatment of meibomian gland dysfunction. Cornea 2012;31:396–404.
[129] Pflugfelder SC, Tseng SC, Sanabria O, Kell H, Garcia CG, Felix C, et al. Evaluation of subjective assessments and objective diagnostic tests for diagnosing tear-film disorders known to cause ocular irritation. Cornea 1998;17:38–56.

[130] Meadows JF, Ramamoorthy P, Nichols JJ, Nichols KK. Development of the 4–3–2–1 Meibum Expressibility Scale. Eye & Contact Lens: Science & Clinical Practice 2012;38:86–92. https://doi.org/10.1097/icl.0b013e318242b494.
[131] Martín-Montañez V, López-de la Rosa A, López-Miguel A, Pinto-Fraga J, González-Méijome JM, González-García MJ. End-of-day dryness, corneal sensitivity and blink rate in contact lens wearers. Cont Lens Anterior Eye 2015;38:148–51.
[132] Bentivoglio AR, Bressman SB, Cassetta E, Carretta D, Tonali P, Albanese A. Analysis of blink rate patterns in normal subjects. Mov Disord 1997;12:1028–34.
[133] Argilés M, Cardona G, Pérez-Cabré E, Rodríguez M. Blink Rate and Incomplete Blinks in Six Different Controlled Hard-Copy and Electronic Reading Conditions. Invest Ophthalmol Vis Sci 2015;56:6679–85.
[134] Van Slooten JC, Jahfari S, Theeuwes J. Spontaneous eye blink rate predicts individual differences in exploration and exploitation during reinforcement learning. Sci Rep 2019;9:17436.
[135] Ousler GW 3rd, Abelson MB, Johnston PR, Rodriguez J, Lane K, Smith LM. Blink patterns and lid-contact times in dry-eye and normal subjects. Clin Ophthalmol 2014;8:869–74.
[136] Jie Y, Sella R, Feng J, Gomez ML, Afshari NA. Evaluation of incomplete blinking as a measurement of dry eye disease. Ocul Surf 2019;17:440–6.
[137] Su Y, Liang Q, Su G, Wang N, Baudouin C, Labbé A. Spontaneous Eye Blink Patterns in Dry Eye: Clinical Correlations. Invest Ophthalmol Vis Sci 2018;59:5149–56.
[138] Schlote T, Kadner G, Freudenthaler N. Marked reduction and distinct patterns of eye blinking in patients with moderately dry eyes during video display terminal use. Graefes Arch Clin Exp Ophthalmol 2004;242:306–12.
[139] Abusharha AA. Changes in blink rate and ocular symptoms during different reading tasks. Clin Optom (Auckl) 2017;9:133–8.
[140] Andreu-Sánchez C, Martín-Pascual MÁ, Gruart A, Delgado-García JM. Looking at reality versus watching screens: Media professionalization effects on the spontaneous eyeblink rate. PLoS One 2017;12:e0176030.
[141] York M, Ong J, Robbins JC. Variation in blink rate associated with contact lens wear and task difficulty. Am J Optom Arch Am Acad Optom 1971;48:461–7.
[142] Rodriguez JD, Lane KJ, Ousler GW 3rd, Angjeli E, Smith LM, Abelson MB. Blink: Characteristics, Controls, and Relation to Dry Eyes. Curr Eye Res 2018;43:52–66.
[143] Jiang X, Tien G, Huang D, Zheng B, Atkins MS. Capturing and evaluating blinks from video-based eyetrackers. Behav Res Methods 2013;45:656–63.
[144] Kawashima M, Tsubota K. Tear lipid layer deficiency associated with incomplete blinking: a case report. BMC Ophthalmol 2013;13:34.
[145] Navascues-Cornago M, Morgan PB, Maldonado-Codina C, Read ML. Characterisation of blink dynamics using a high-speed infrared imaging system. Ophthalmic Physiol Opt 2020;40:519–28.
[146] McMonnies CW. Incomplete blinking: exposure keratopathy, lid wiper epitheliopathy, dry eye, refractive surgery, and dry contact lenses. Cont Lens Anterior Eye 2007;30:37–51.
[147] Wang MTM, Tien L, Han A, Lee JM, Kim D, Markoulli M, et al. Impact of blinking on ocular surface and tear film parameters. Ocul Surf 2018;16:424–9.
[148] Wang MTM, Muntz A, Lim J, Kim JS, Lacerda L, Arora A, et al. Ageing and the natural history of dry eye disease: A prospective registry-based cross-sectional study. Ocul Surf 2020. https://doi.org/10.1016/j.jtos.2020.07.003.
[149] Portello JK, Rosenfield M, Chu CA. Blink rate, incomplete blinks and computer vision syndrome. Optom Vis Sci 2013;90:482–7.
[150] Ousler GW, Hagberg KW, Schindelar M, Welch D, Abelson MB. The Ocular Protection Index. Cornea 2008;27:509–13. https://doi.org/10.1097/ico.0b013e31816583f6.
[151] Ousler GW, Michaelson C, Christensen MT. An evaluation of tear film breakup time extension and ocular protection index scores among three marketed lubricant eye drops. Cornea 2007;26:949–52.

[152] Lyons CJ, McNab AA. Symptomatic nocturnal lagophthalmos. Aust N Z J Ophthalmol 1990;18:393–6.
[153] Blackie CA, Korb DR. A novel lid seal evaluation: the Korb-Blackie light test. Eye Contact Lens 2015;41:98–100.
[154] Thomas R, Thomas S, Braganza A, Muliyil J. Evaluation of the role of syringing prior to cataract surgery. Indian J Ophthalmol 1997;45:211–4.
[155] Kashkouli MB, Abolfathzadeh N, Abdolalizadeh P, Karimi N, Hedayati R, Jafari S, et al. How reliable is the lacrimal scintigraphy report? An inter-observer agreement and reliability study. Int J Ophthalmol 2019;12:401–6.
[156] Kashkouli MB, Pakdel F, Kiavash V. Assessment and management of proximal and incomplete symptomatic obstruction of the lacrimal drainage system. Middle East Afr J Ophthalmol 2012;19:60–9.
[157] Dutton JJ, White JJ. Imaging and Clinical Evaluation of the Lacrimal Drainage System. In: Cohen AJ, Mercandetti M, Brazzo BG, editors. The Lacrimal System, New York: Springer; 2006, p. 74–95.
[158] Eperjesi F, Bartlett H, Dunne M. Examination of the external and anterior structures. Ophthalmic Clinical Procedures 2007:95–6. https://doi.org/10.1016/b978-0-08-044978-4.50032-0.
[159] Müllner K, Bodner E, Mannor GE. Endoscopy of the lacrimal system. Br J Ophthalmol 1999;83:949–52.
[160] Das S. Evaluation of Epiphora. In: Ali MJ, editor. Principles and Practice of Lacrimal Surgery, Singapore: Springer Singapore; 2018, p. 69–82.
[161] Elmorsy SM, Fayk HM. Nasal endoscopic assessment of failure after external dacryocystorhinostomy. Orbit 2010;29:197–201.
[162] Saleh H, Choudhury N. Nasal Endoscopic Evaluation. In: Ali MJ, editor. Principles and Practice of Lacrimal Surgery, Singapore: Springer Singapore; 2018, p. 91–6.
[163] Ali MJ. Newer Endoscopes and Three-Dimensional Nasal Endoscopy. In: Ali MJ, editor. Principles and Practice of Lacrimal Surgery, Singapore: Springer Singapore; 2018, p. 97–101.
[164] Murai S. Measurement with nasal scintigraphy of nasal mucociliary clearance in normal man. Jibi To Rinsho 1989;82:457–70.
[165] Craig JP, Nichols KK, Akpek EK, Caffery B, Dua HS, Joo C-K, et al. TFOS DEWS II Definition and Classification Report. Ocul Surf 2017;15:276–83.
[166] Pult H, Wolffsohn JS. The development and evaluation of the new Ocular Surface Disease Index-6. Ocul Surf 2019;17:817–21.
[167] Wang MTM, Xue AL, Craig JP. Screening utility of a rapid non-invasive dry eye assessment algorithm. Cont Lens Anterior Eye 2019;42:497–501.
[168] Stapleton F, Alves M, Bunya VY, Jalbert I, Lekhanont K, Malet F, et al. TFOS DEWS II Epidemiology Report. Ocul Surf 2017;15:334–65.
[169] Dumbleton K, Caffery B, Dogru M, Hickson-Curran S, Kern J, Kojima T, et al. The TFOS International Workshop on Contact Lens Discomfort: report of the subcommittee on epidemiology. Invest Ophthalmol Vis Sci 2013;54:TFOS20–36.
[170] Pucker AD, Dougherty BE, Jones-Jordan LA, Kwan JT, Kunnen CME, Srinivasan S. Psychometric Analysis of the SPEED Questionnaire and CLDEQ-8. Invest Ophthalmol Vis Sci 2018;59:3307–13.
[171] López-de la Rosa A, Arroyo-Del Arroyo C, Enríquez-de-Salamanca A, Pinto-Fraga J, López-Miguel A, González-García MJ. The ability of the Contact Lens Dry Eye Questionnaire (CLDEQ)-8 to detect ocular surface alterations in contact lens wearers. Cont Lens Anterior Eye 2019;42:273–7.
[172] Chalmers RL, Keay L, Hickson-Curran SB, Gleason WJ. Cutoff score and responsiveness of the 8-item Contact Lens Dry Eye Questionnaire (CLDEQ-8) in a Large daily disposable contact lens registry. Cont Lens Anterior Eye 2016;39:342–52.
[173] Bron AJ, de Paiva CS, Chauhan SK, Bonini S, Gabison EE, Jain S, et al. TFOS DEWS II pathophysiology report. Ocul Surf 2017;15:438–510.
[174] Craig JP, Tomlinson A. Effect of age on tear osmolality. Optom Vis Sci 1995;72:713–7.

[175] Tiffany JM, Chew CKS, Bron AJ. VAPOR-PRESSURE OSMOMETRY OF HUMAN TEARS. INVESTIGATIVE OPHTHALMOLOGY & VISUAL SCIENCE, vol. 35, LIPPINCOTT-RAVEN PUBL 227 EAST WASHINGTON SQ, PHILADELPHIA, PA 19106; 1994, p. 1692–1692.
[176] Lemp MA, Bron AJ, Baudouin C, Benítez del Castillo JM, Geffen D, Tauber J, et al. Tear Osmolarity in the Diagnosis and Management of Dry Eye Disease. Am J Ophthalmol 2011;151:792–8.e1.
[177] Tomlinson A, McCann LC, Pearce EI. Comparison of human tear film osmolarity measured by electrical impedance and freezing point depression techniques. Cornea 2010;29:1036–41.
[178] Bunya VY, Fuerst NM, Pistilli M, McCabe BE, Salvo R, Macchi I, et al. Variability of Tear Osmolarity in Patients With Dry Eye. JAMA Ophthalmol 2015;133:662–7.
[179] Downie LE, Vingrys AJ. Accuracy of Laboratory Assays in Ophthalmic Practice. JAMA Ophthalmol 2015;133:1480.
[180] Murube J. Tear osmolarity. Ocul Surf 2006;4:62–73.
[181] Liu H, Begley C, Chen M, Bradley A, Bonanno J, McNamara NA, et al. A link between tear instability and hyperosmolarity in dry eye. Invest Ophthalmol Vis Sci 2009;50:3671–9.
[182] Versura P, Campos EC. TearLab® Osmolarity System for diagnosing dry eye. Expert Rev Mol Diagn 2013;13:119–29.
[183] Gad A, Vingrys AJ, Wong CY, Jackson DC, Downie LE. Tear film inflammatory cytokine upregulation in contact lens discomfort. Ocul Surf 2019;17:89–97.
[184] Keech A, Senchyna M, Jones L. Impact of time between collection and collection method on human tear fluid osmolarity. Curr Eye Res 2013;38:428–36.
[185] Sullivan BD, Pepose JS, Foulks GN. Progressively Increased Variation in Tear Osmolarity Mirrors Dry Eye Severity. JAMA Ophthalmol 2015;133:1481–2.
[186] Wang MTM, Ormonde SE, Muntz A, Craig JP. Diagnostic profile of tear osmolarity and inter-ocular variability for dry eye disease. Clin Experiment Ophthalmol 2020;48:255–7.
[187] Yamamoto Y, Yokoi N, Higashihara H, Inagaki K, Sonomura Y, Komuro A, et al. Clinical characteristics of short tear film breakup time (BUT)-type dry eye. Nihon Ganka Gakkai Zasshi 2012;116:1137–43.
[188] Xue AL, Downie LE, Ormonde SE, Craig JP. A comparison of the self-reported dry eye practices of New Zealand optometrists and ophthalmologists. Ophthalmic Physiol Opt 2017;37:191–201.
[189] Downie LE, Keller PR, Vingrys AJ. An Evidence-Based Analysis of Australian Optometrists' Dry Eye Practices. Optometry and Vision Science 2013;90:1385–95. https://doi.org/10.1097/opx.0000000000000087.
[190] Downie LE, Rumney N, Gad A, Keller PR, Purslow C, Vingrys AJ. Comparing self-reported optometric dry eye clinical practices in Australia and the United Kingdom: is there scope for practice improvement? Ophthalmic Physiol Opt 2016;36:140–51.
[191] Norn MS. Desiccation of the precorneal film. I. Corneal wetting-time. Acta Ophthalmol 1969;47:865–80.
[192] Mooi JK, Wang MTM, Lim J, Müller A, Craig JP. Minimising instilled volume reduces the impact of fluorescein on clinical measurements of tear film stability. Cont Lens Anterior Eye 2017;40:170–4.
[193] Cho P, Douthwaite W. The relation between invasive and noninvasive tear break-up time. Optom Vis Sci 1995;72:17–22.
[194] Sweeney DF, Millar TJ, Raju SR. Tear film stability: a review. Exp Eye Res 2013;117:28–38.
[195] Downie LE, Keller PR. A Pragmatic Approach to Dry Eye Diagnosis. Optometry and Vision Science 2015;92:1189–97. https://doi.org/10.1097/opx.0000000000000721.
[196] Mengher LS, Bron AJ, Tonge SR, Gilbert DJ. A non-invasive instrument for clinical assessment of the pre-corneal tear film stability. Curr Eye Res 1985;4:1–7.
[197] Patel S, Murray D, McKenzie A, Shearer DS, McGrath BD. Effects of fluorescein on tear breakup time and on tear thinning time. Am J Optom Physiol Opt 1985;62:188–90.

[198] Bandlitz S, Peter B, Pflugi T, Jaeger K, Anwar A, Bikhu P, et al. Agreement and repeatability of four different devices to measure non-invasive tear breakup time (NIBUT). Cont Lens Anterior Eye 2020. https://doi.org/10.1016/j.clae.2020.02.018.
[199] Kim J, Kim JY, Seo KY, Kim T-I, Chin HS, Jung JW. Location and pattern of non-invasive keratographic tear film break-up according to dry eye disease subtypes. Acta Ophthalmol 2019;97:e1089–97.
[200] Craig JP, Tomlinson A. Importance of the lipid layer in human tear film stability and evaporation. Optom Vis Sci 1997;74:8–13.
[201] Guillon JP. Non-invasive Tearscope Plus routine for contact lens fitting. Cont Lens Anterior Eye 1998;21 Suppl 1:S31–40.
[202] Wang MTM, Jaitley Z, Lord SM, Craig JP. Comparison of Self-applied Heat Therapy for Meibomian Gland Dysfunction. Optom Vis Sci 2015;92:e321–6.
[203] Wang MTM, Dean SJ, Muntz A, Craig JP. Evaluating the diagnostic utility of evaporative dry eye disease markers. Clin Experiment Ophthalmol 2020;48:267–70.
[204] Finis D, Pischel N, Schrader S, Geerling G. Evaluation of lipid layer thickness measurement of the tear film as a diagnostic tool for Meibomian gland dysfunction. Cornea 2013;32:1549–53.
[205] Markoulli M, Duong TB, Lin M, Papas E. Imaging the Tear Film: A Comparison Between the Subjective Keeler Tearscope-Plus™ and the Objective Oculus® Keratograph 5M and LipiView® Interferometer. Curr Eye Res 2018;43:155–62.
[206] Mishima S, Gasset A, Klyce SD Jr, Baum JL. Determination of tear volume and tear flow. Invest Ophthalmol 1966;5:264–76.
[207] Xu KP, Tsubota K. Correlation of tear clearance rate and fluorophotometric assessment of tear turnover. Br J Ophthalmol 1995;79:1042–5.
[208] Kuppens EV, Stolwijk TR, de Keizer RJ, van Best JA. Basal tear turnover and topical timolol in glaucoma patients and healthy controls by fluorophotometry. Invest Ophthalmol Vis Sci 1992;33:3442–8.
[209] Willcox MDP, Argueso P, Georgiev GA, Holopainen JM, Laurie GW, Millar TJ, et al. TFOS DEWS II Tear Film Report. Ocul Surf 2017;15:366–403.
[210] Cho P, Yap M. Schirmer test. I. A review. Optom Vis Sci 1993;70:152–6.
[211] Miller WL, Doughty MJ, Narayanan S, Leach NE, Tran A, Gaume AL, et al. A comparison of tear volume (by tear meniscus height and phenol red thread test) and tear fluid osmolality measures in non-lens wearers and in contact lens wearers. Eye Contact Lens 2004;30:132–7.
[212] Hamano H, Hori M, Hamano T, Mitsunaga S, Maeshima J, Kojima S, et al. A new method for measuring tears. CLAO J 1983;9:281–9.
[213] Pult H, Purslow C, Murphy PJ. The relationship between clinical signs and dry eye symptoms. Eye 2011;25:502–10.
[214] de Monchy I, Gendron G, Miceli C, Pogorzalek N, Mariette X, Labetoulle M. Combination of the Schirmer I and phenol red thread tests as a rescue strategy for diagnosis of ocular dryness associated with Sjögren's syndrome. Invest Ophthalmol Vis Sci 2011;52:5167–73.
[215] Tomlinson A, Blades KJ, Pearce EI. What does the phenol red thread test actually measure? Optom Vis Sci 2001;78:142–6.
[216] Kashkouli MB, Pakdel F, Amani A, Asefi M, Aghai GH, Falavarjani KG. A modified Schirmer test in dry eye and normal subjects: open versus closed eye and 1-minute versus 5-minute tests. Cornea 2010;29:384–7.
[217] Holly FJ. Physical chemistry of the normal and disordered tear film. Trans Ophthalmol Soc U K 1985;104 (Pt 4):374–80.
[218] Savini G, Barboni P, Zanini M. Tear meniscus evaluation by optical coherence tomography. Ophthalmic Surg Lasers Imaging 2006;37:112–8.
[219] Gaffney EA, Tiffany JM, Yokoi N, Bron AJ. A mass and solute balance model for tear volume and osmolarity in the normal and the dry eye. Prog Retin Eye Res 2009. https://doi.org/S1350-9462(09)00071-8 [pii].

[220] Palakuru JR, Wang J, Aquavella JV. Effect of blinking on tear dynamics. Invest Ophthalmol Vis Sci 2007;48:3032–7.
[221] Yokoi N, Bron AJ, Tiffany JM, Maruyama K, Komuro A, Kinoshita S. Relationship between tear volume and tear meniscus curvature. Arch Ophthalmol 2004;122:1265–9.
[222] Golding TR, Bruce AS, Mainstone JC. Relationship between tear-meniscus parameters and tear-film breakup. Cornea 1997;16:649–61.
[223] Mainstone JC, Bruce AS, Golding TR. Tear meniscus measurement in the diagnosis of dry eye. Curr Eye Res 1996;15:653–61.
[224] Oguz H, Yokoi N, Kinoshita S. The height and radius of the tear meniscus and methods for examining these parameters. Cornea 2000;19:497–500.
[225] Johnson ME, Murphy PJ. The agreement and repeatability of tear meniscus height measurement methods. Optom Vis Sci 2005;82:1030–7.
[226] Bandlitz S, Purslow C, Murphy PJ, Pult H. Comparison of a new portable digital meniscometer and optical coherence tomography in tear meniscus radius measurement. Acta Ophthalmol 2014;92:e112–8.
[227] Czajkowski G, Kaluzny BJ, Laudencka A, Malukiewicz G, Kaluzny JJ. Tear meniscus measurement by spectral optical coherence tomography. Optom Vis Sci 2012;89:336–42.
[228] Arita R, Yabusaki K, Hirono T, Yamauchi T, Ichihashi T, Fukuoka S, et al. Automated Measurement of Tear Meniscus Height with the Kowa DR-1α Tear Interferometer in Both Healthy Subjects and Dry Eye Patients. Invest Ophthalmol Vis Sci 2019;60:2092–101.
[229] Stegmann H, Werkmeister RM, Pfister M, Garhöfer G, Schmetterer L, Dos Santos VA. Deep learning segmentation for optical coherence tomography measurements of the lower tear meniscus. Biomed Opt Express 2020;11:1539–54.
[230] Li J, Shen M, Wang J, Ma H, Tao A, Xu S, et al. Clinical significance of tear menisci in dry eye. Eye Contact Lens 2012;38:183–7.
[231] Santodomingo-Rubido J, Wolffsohn JS, Gilmartin B. Comparison between graticule and image capture assessment of lower tear film meniscus height. Cont Lens Anterior Eye 2006;29:169–73.
[232] Johnson ME, Murphy PJ. Temporal changes in the tear menisci following a blink. Exp Eye Res 2006;83:517–25.
[233] Bandlitz S, Purslow C, Murphy PJ, Pult H. Influence of conjunctival folds on calculated lower tear meniscus volume. Contact Lens and Anterior Eye 2018;41:S9–10. https://doi.org/10.1016/j.clae.2018.04.108.
[234] Bandlitz S, Purslow C, Murphy PJ, Pult H. Tear meniscus regularity along the lower eyelid. Contact Lens and Anterior Eye 2013;36:e3. https://doi.org/10.1016/j.clae.2013.08.016.
[235] Srinivasan S, Chan C, Jones L. Apparent time-dependent differences in inferior tear meniscus height in human subjects with mild dry eye symptoms. Clin Exp Optom 2007;90:345–50.
[236] Afonso AA, Monroy D, Stern ME, Feuer WJ, Tseng SC, Pflugfelder SC. Correlation of tear fluorescein clearance and Schirmer test scores with ocular irritation symptoms. Ophthalmology 1999;106:803–10.
[237] Macri A, Rolando M, Pflugfelder S. A standardized visual scale for evaluation of tear fluorescein clearance. Ophthalmology 2000;107:1338–43.
[238] Pearce EI, Keenan BP, McRory C. An improved fluorophotometric method for tear turnover assessment. Optom Vis Sci 2001;78:30–6.
[239] Zheng X, Kamao T, Yamaguchi M, Sakane Y, Goto T, Inoue Y, et al. New method for evaluation of early phase tear clearance by anterior segment optical coherence tomography. Acta Ophthalmol 2014;92:e105–11.
[240] Garaszczuk IK, Mousavi M, Cervino Exposito A, Bartuzel MM, Montes-Micó R, Iskander DR. Evaluating tear clearance rate with optical coherence tomography. Cont Lens Anterior Eye 2018;41:54–9.